

## Precise Dynamical Masses and Orbital Fits for $\beta$ Pic b and $\beta$ Pic c

G. MIREK BRANDT <sup>1,\*</sup>, TIMOTHY D. BRANDT <sup>1</sup>, TRENT J. DUPUY <sup>2</sup>, YITING LI <sup>1</sup> AND DANIEL MICHALIK <sup>3,†</sup>

<sup>1</sup>*Department of Physics, University of California, Santa Barbara, Santa Barbara, CA 93106, USA*

<sup>2</sup>*Institute for Astronomy, University of Edinburgh, Royal Observatory, Blackford Hill, Edinburgh, EH9 3HJ, UK*

<sup>3</sup>*European Space Agency (ESA), European Space Research and Technology Centre (ESTEC), Keplerlaan 1, 2201 AZ Noordwijk, The Netherlands*

(Received Nov 11, 2020)

Submitted to AJ

### ABSTRACT

We present precise dynamical masses and orbital fits to the exoplanets  $\beta$  Pictoris b and c. We find a mass of  $9.8_{-2.6}^{+2.7} M_{\text{Jup}}$  for  $\beta$  Pic b and  $8.3_{-1.0}^{+1.1} M_{\text{Jup}}$  for  $\beta$  Pic c with uniform priors on both. We use fifteen years of radial velocities and relative astrometry, including recent GRAVITY measurements, absolute astrometry from *Hipparcos* and *Gaia*, and a single relative RV measurement between  $\beta$  Pic A and b. We find a good fit using the orbit code `orvara` with a well-constrained eccentricity of  $0.121 \pm 0.008$  for  $\beta$  Pic b, and a poorly constrained eccentricity of  $0.30_{-0.16}^{+0.20}$  for  $\beta$  Pic c, with the two orbital planes aligned to within  $\sim 0.5^\circ$ . Both planets' masses are within  $\sim 1\sigma$  of the predictions of hot-start evolutionary models and exclude cold starts. We validate our approach on  $N$ -body synthetic data integrated using REBOUND. We show that `orvara` can account for three-body effects in the  $\beta$  Pic system down to a level  $\sim 5$  times smaller than the GRAVITY uncertainties. Systematics in the masses and orbital parameters from `orvara`'s approximate treatment of multiplanet orbits are a factor of  $\sim 5$  smaller than the uncertainties we derive here. Future GRAVITY observations will improve the constraints on  $\beta$  Pic c's mass and (especially) eccentricity, but improved constraints on the mass of  $\beta$  Pic b will likely require years of additional RV monitoring and improved precision from future *Gaia* data releases.

*Keywords:* —

### 1. INTRODUCTION

$\beta$  Pictoris b ( $\beta$  Pic b) was among the first exoplanets to be directly imaged (Lagrange et al. 2010). Since then, it has been observed dozens of times, resulting in photometry spanning the near-infrared (Quanz et al. 2010; Bonnefoy et al. 2011; Currie et al. 2011; Bonnefoy et al. 2013; Males et al. 2014), low-resolution spectroscopy (Chilcote et al. 2015, 2017), and even medium-resolution spectroscopy (Snellen et al. 2014; Gravity Collaboration et al. 2020). Part of the system's importance derives from the well-measured age of  $\beta$  Pic A. The host star is the defining, highest-mass member of the  $\beta$  Pictoris moving group (Barrado y Navascués et al. 1999; Zucker- man et al. 2001), which has concordant age determinations of  $\sim 20$  million years (Myr) from lithium depletion boundary measurements (Binks & Jeffries 2014; Shkol-

nik et al. 2012), isochrone analysis (Bell et al. 2015), and kinematic traceback (Miret-Roig et al. 2020).

Combining this well-measured age with an independently measured mass and luminosity can constrain  $\beta$  Pic b's initial supply of thermal energy and provide clues to  $\beta$  Pic b's formation mechanism (Marley et al. 2007; Fortney et al. 2008; Spiegel & Burrows 2012; Marleau & Cumming 2014).

Dynamical mass measurements of  $\beta$  Pic b became feasible thanks to absolute astrometry from the *Hipparcos* (ESA 1997; van Leeuwen 2007) and *Gaia* (Gaia Collaboration et al. 2016; Lindgren et al. 2018) missions. Since *Gaia*'s second data release, a number of authors derived masses and orbits of  $\sim 10$ – $15 M_{\text{Jup}}$  (Snellen & Brown 2018; Dupuy et al. 2019; Nielsen et al. 2020). The picture was recently complicated and enriched by the discovery of a second companion,  $\beta$  Pic c, orbiting roughly 3 AU from the host star (Lagrange et al. 2019a; Nowak et al. 2020), interior to the  $\approx 10$  AU orbit

\* NSF Graduate Research Fellow

† ESA Research Fellow

of  $\beta$  Pic b. Precision astrometry from the GRAVITY instrument can now resolve the influence of  $\beta$  Pic c on the relative orbit of  $\beta$  Pic b around  $\beta$  Pic A (Nowak et al. 2020; Lagrange et al. 2020).

Nowak et al. (2020) and Lagrange et al. (2020) recently fit a two-planet Keplerian model to the  $\beta$  Pic system. When these authors adopted an uninformative prior on the mass of  $\beta$  Pic b, their best-fit dynamical mass measurements were  $3.2 M_{\text{Jup}}$  (Lagrange et al. 2020) and  $5.6 \pm 1.5 M_{\text{Jup}}$  (Nowak et al. 2020). As the authors noted, such low masses are incompatible with cooling models. Cooling models predict much higher masses that are needed to produce the observed flux (e.g., Baraffe et al. 2003; Spiegel & Burrows 2012). Nowak et al. (2020) ultimately adopted a prior of  $15 \pm 3 M_{\text{Jup}}$  while Lagrange et al. (2020) used a prior of  $14 \pm 1 M_{\text{Jup}}$ . With these priors, the posterior masses are shifted to near  $\sim 10 M_{\text{Jup}}$ . The necessity to use such an informative prior indicates a tension between the dynamical constraints and model predictions from spectral analyses, as noted by Nowak et al. (2020).

In this paper, we present precise masses and orbits of  $\beta$  Pic b and  $\beta$  Pic c without the need for informative priors on the planets’ masses. Our inferred masses are compatible with a range of cooling model predictions. We structure the paper as follows. In Section 2, we describe the data that we adopt and the method that we use to fit the system’s orbit; we include a full validation on a synthetic data set produced using  $N$ -body integration. We present our results in Section 3, including the masses and orbital parameters of both planets, an assessment of the relative astrometry, predicted positions of  $\beta$  Pic b and  $\beta$  Pic c, and  $N$ -body results. We discuss the details and implications of our work in Section 4. We summarize our results and conclude in Section 5.

## 2. DATA AND FITTING

### 2.1. Data

The available data for the  $\beta$  Pic system comprise more than 15 years of radial velocities (RVs) of  $\beta$  Pic A and relative astrometry for  $\beta$  Pic b, three epochs of relative astrometry for  $\beta$  Pic c, a single RV of  $\beta$  Pic b relative to  $\beta$  Pic A, and absolute astrometry of  $\beta$  Pic A from *Hipparcos* and *Gaia*. In this section we summarize each of these.

There are several sources and numerous measurements of relative astrometry for  $\beta$  Pic b, and three recent measurements for  $\beta$  Pic c. We use all relative astrometry, except for that from VLT/SPHERE (Lagrange et al. 2019b). Nielsen et al. (2020) identified a systematic offset in position angle (PA) and we find evidence for an offset in separation (see Section 3). The relative as-

trometry we use comprises measurements from NICI on Gemini-South (Nielsen et al. 2014), NACO on the VLT (Currie et al. 2011; Chauvin et al. 2012), MagAO on Magellan (Nielsen et al. 2014), GPI on Gemini South (Wang et al. 2016; Nielsen et al. 2020), and GRAVITY on the VLT (7 on  $\beta$  Pic b, 3 on c) (Lagrange et al. 2020; Nowak et al. 2020). This corresponds to the Case 3 relative astrometry data set of Nielsen et al. (2020) plus recent observations by GRAVITY.

GRAVITY measurements of  $\beta$  Pic b clustered near 2020 disagree internally by  $\sim 2\sigma$  and result in an unacceptable reduced  $\chi^2$  (near 3) on PA in the final fit (see Section 3.2). We therefore inflate the errors on the seven GRAVITY measurements of  $\beta$  Pic b by a factor of two to make the PA reduced  $\chi^2$  acceptable and bring the PA of the 2020 measurements into internal agreement.

We use the RVs of  $\beta$  Pic A as presented in Vandal et al. (2020), which are corrected for pulsations via a Gaussian Process. We add the five new RVs presented in Lagrange et al. (2020) that are not in the data set of Vandal et al. (2020).<sup>1</sup> We also use the single measurement of the relative RV of  $\beta$  Pic b and  $\beta$  Pic A from Snellen et al. (2014).

We use the absolute astrometry of the *Hipparcos-Gaia* Catalog of Accelerations (HGCA, Brandt 2018). These astrometric measurements adopt the *Gaia* DR2 parallax values as priors to all *Hipparcos* data. *Gaia* is usually much more precise than *Hipparcos*, but  $\beta$  Pic A is at the saturation limit of *Gaia* ( $G$ -band magnitude of 3.7). This strongly impacts the astrometric performance of *Gaia* (Lindgren et al. 2018). Thus, the formal parallax uncertainties of the two missions are comparable (assuming a substantial error inflation to the parallax of the *Hipparcos* re-reduction in line with the HGCA’s inflation of proper motion errors). Because the HGCA adopts *Gaia* parallaxes as a prior, we take the *Gaia* DR2 parallax value of  $50.62 \pm 0.33$  milli-arcseconds (mas) (Lindgren et al. 2018) as our prior for the orbital fit. This value is consistent to within 1% with the *Hipparcos* values (ESA 1997; van Leeuwen 2007). Regardless, the precise distance to  $\beta$  Pic does not drive our results.

The HGCA argues for a factor of  $\sim 2$  inflation for all *Gaia* DR2 proper motion errors. We further inflate the HGCA *Gaia* DR2 proper motion errors on  $\beta$  Pic by another factor of 2 (a net factor of  $\sim 4$  over the *Gaia* DR2 errors). This is due to systematics in the astrometric fit for very bright stars and is justified by the black histogram (worst 5% of stars) in Figure 9 of Brandt (2018).

<sup>1</sup> The RVs between Vandal et al. (2020) and Lagrange et al. (2020) agree within the errors for the epochs mutual to the two data sets.

The *Gaia* DR2 proper motion has a negligible impact on our results with this large error inflation.

### 2.2. Orbit Code

We use `orvara` (Brandt et al. 2020, submitted) along with `htof` (Brandt et al. 2020, submitted; Brandt & Michalik 2020) to fit for the motion of the  $\beta$  Pic system. `orvara` fits one or more Keplerian orbits to an arbitrary combination of RVs, relative, and absolute astrometry. For the present analysis, we added the ability to fit the single relative RV measurement by Snellen et al. (2014). `orvara` treats the full motion of the system as a linear combination of Keplerian orbits: an orbit between  $\beta$  Pic b and the combined  $\beta$  Pic A/c system, and a second Keplerian orbit between  $\beta$  Pic A and  $\beta$  Pic c. When computing relative astrometry between  $\beta$  Pic A and  $\beta$  Pic c, `orvara` neglects interactions with  $\beta$  Pic b. For relative astrometry between  $\beta$  Pic A and  $\beta$  Pic b, `orvara` computes the displacement of  $\beta$  Pic A from its center of mass with  $\beta$  Pic c and adds this to the displacement of  $\beta$  Pic b from the center of mass of the  $\beta$  Pic A/c system. In other words, `orvara` only adds astrometric perturbations due to inner companions, not due to outer companions. For RVs and absolute astrometry of  $\beta$  Pic A, `orvara` adds the perturbations from the two Keplerian orbits. The perturbation from planet c on the relative RV measurement is negligible.

`orvara` uses `htof` to derive positions and proper motions from synthetic epoch astrometry relative to the system’s barycenter. `htof` uses the known *Hipparcos* observation times and scan angles and the predicted *Gaia* observation times and scan angles<sup>2</sup> (with dead times removed) and solves for the best-fit position and proper motion relative to the barycenter. `orvara` then compares these positions and proper motions to the equivalent values in the HGCA.

`orvara` marginalizes out the RV zero point, the parallax, and the barycenter proper motion. We fit a total of 16 parameters to the system using Markov Chain Monte Carlo (MCMC) with `ptemcee` (Foreman-Mackey et al. 2013; Vausden et al. 2016). These are the six Keplerian orbital elements for each of planets b and c, the mass of each companion, the mass of  $\beta$  Pic A, and a RV jitter to be added in quadrature with the RV uncertainties. We adopt uninformative priors on all parameters: uniform priors on all parameters except for RV jitter (a log-uniform prior) and inclination (a geometric prior).

### 2.3. Validation

<sup>2</sup> <https://gaia.esac.esa.int/gost/>

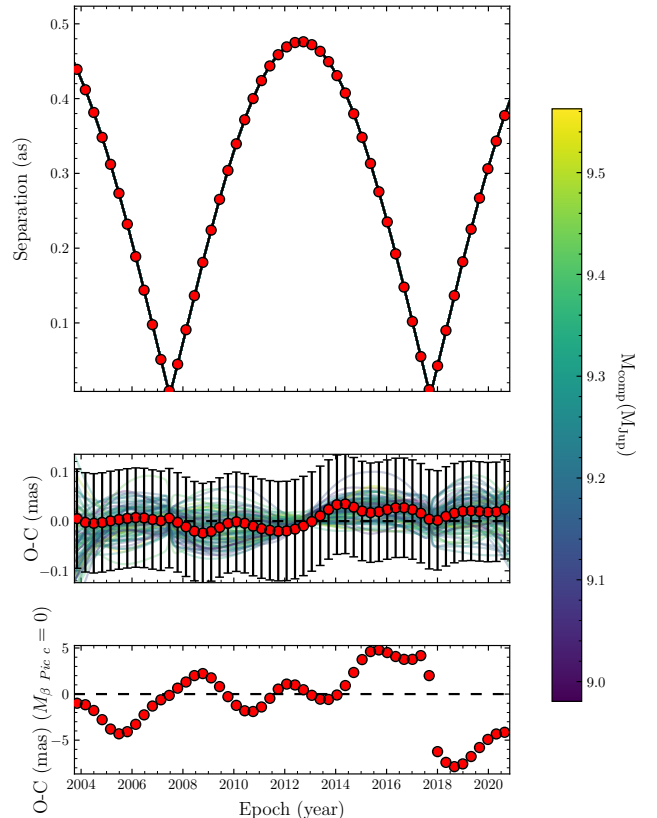


**Figure 1.** `orvara` can fit the 3-body system of  $\beta$  Pic to several factors below the GRAVITY precision (assumed to be 0.1 mas). Top panel: the observed separation for the fictitious  $\beta$  Pic b analog with evenly spaced observations with the precision of GRAVITY as presented in Lagrange et al. (2020). Black is the best fit orbit found by an `orvara` MCMC analysis. Middle panel: observed data minus the best fit orbit (O-C). The remaining variations are from the mutual tugs of  $\beta$  Pic c on  $\beta$  Pic b. These variations are at the level of  $\sim 0.02$  mas – a factor of 5 below the 0.1 mas precision of the GRAVITY-like data. Bottom panel: the O-C if the approximate 3-body compensation is turned off in `orvara`. The synthetic data here are generated with a  $9 M_{\text{Jup}}$   $\beta$  Pic b and the best-fit mass is  $9.2 M_{\text{Jup}}$ .

Given the approximate treatment of the three-body problem in `orvara`, we test its fidelity on data integrated forward using `REBOUND` (Rein & Liu 2012). We initialize a  $1.8 M_{\odot}$  star with two planets of 9 and  $8 M_{\text{Jup}}$ ; we give these planets the best-fit orbital elements of  $\beta$  Pic b and c, respectively, found by Lagrange et al. (2020). We then integrate the system forward to produce synthetic RVs and relative astrometry for both companions with `REBOUND`. We take 52 measurements of relative astrometry for each planet distributed over 17 years, each of which has the  $100 \mu\text{as}$  precision typical of GRAVITY (Gravity Collaboration et al. 2020; Lagrange et al. 2020). We fit 52 RV points, each with an uncertainty of 1 m/s.

We add a single relative RV between  $\beta$  Pic b and A (the synthetic analog to the relative RV of Snellen et al. (2014)) with an uncertainty of 1 km/s. We then fit these synthetic data with `orvara`.

`orvara` is able to fit all data satisfactorily. Figure 1 shows that the unmodeled three-body effects are a factor of  $\sim 5$  below the level detectable by GRAVITY (see middle panel). The superposition of the two Keplerian orbits shows up in the relative astrometry of  $\beta$  Pic b, where synthetic GRAVITY observations clearly detect the orbit of  $\beta$  Pic A about its center of mass with  $\beta$  Pic c (bottom panel of Figure 1). Unmodeled RV residuals are well below 1 m/s (the reduced  $\chi^2$  of the RV fit is 0.05). We derive masses that agree well, but not perfectly, with the input masses: the derived masses of  $\beta$  Pic A and  $\beta$  Pic b are each  $\sim 3\%$  larger than their true values. These systematics are a factor of  $\sim 5$  lower than the uncertainties we derive for  $\beta$  Pic c in the following section and are negligible for  $\beta$  Pic b.

`orvara` returns two body elements for each planet about the star. In the three body system that we initialized in REBOUND, the two-body input orbital elements (semi-major axis, eccentricity, etc.) cease to have a strict meaning unless a primary is specified (e.g., the barycenter or  $\beta$  Pic A). However, we still expect the recovered orbital elements to roughly be equal to those that were used as inputs. We expect the semi-major axes to be close but not exactly equal to the inputs, because, e.g., the input semi-major axis of  $\beta$  Pic b was defined relative to the barycenter of  $\beta$  Pic A and c – yet  $\beta$  Pic b will orbit the total system barycenter during integration. Likewise, we expect the argument and time of periastron to be biased slightly. Elements like the inclination  $i$  and PA of the ascending node  $\Omega$  should be returned *exactly* – the 3-body interactions should not rotate the orientation of either orbit over a  $\sim 20$  year integration.

We find that `orvara` recovers  $i$  and  $\Omega$  exactly; with a residual less than  $10^{-3}$  of a degree (nearly equal to the formal error) on both. Although unexpected, we recover the eccentricity exactly as well: the residual is less than  $10^{-4}$  and the formal error is  $2 \cdot 10^{-4}$ . The three elements recovered with biases follow. The argument of periastron and mean longitude at the reference epoch are recovered to within 0.2 degrees. The semi-major axes of both planets are recovered to within 0.1 A.U.

We conclude that our approximation to the three-body dynamics is more than sufficiently accurate for the  $\beta$  Pic system: the biases induced in the parameters inferred from the test data are much smaller than the formal errors on the measured parameters. Our accounting of only inner companions when perturbing relative as-

trometry recovers the masses to within a few percent. Figure 1 shows that a full  $N$ -body integration of the  $\beta$  Pic system will remain unnecessary even with future GRAVITY relative astrometry.

### 3. RESULTS

We infer masses and orbital parameters using a parallel-tempered MCMC with 15 temperatures; for each temperature we use 100 walkers with one million steps per walker.<sup>3</sup> Our MCMC chains converged after 40,000 steps; we conservatively discard the first 250,000 as burn in and use the remainder for inference.<sup>4</sup>

#### 3.1. Orbital Analysis of the $\beta$ Pic System

Table 1 lists the six Keplerian orbital elements for both  $\beta$  Pic b and  $\beta$  Pic c, along with the other five fitted parameters.

Every fitted element of  $\beta$  Pic b results in a nearly Gaussian posterior (see Figure 2). The elements of  $\beta$  Pic c are also well-constrained except for eccentricity and the mean longitude at the reference epoch  $\lambda_{\text{ref}}$ . The mean longitude at the reference epoch is poorly constrained because of the poor constraint on the eccentricity, which results from having only three relative astrometric measurements closely spaced in time. We show the variances and covariances between the fitted parameters in Figure 3 for  $\beta$  Pic c as a corner plot. There is a modest covariance between semi-major axis and eccentricity resulting from the short time baseline of relative astrometry on  $\beta$  Pic c.

The best-fit orbit and nearby (in parameter space) orbits agree well with all data: the pulsation-corrected RVs, the Snellen et al. (2014) relative RV, the relative astrometry from VLT/NACO, Gemini-South/NICI, Magellan/MagAO, Gemini-South/GPI, and GRAVITY, and absolute astrometry from the HGCA.

Figure 4 shows the agreement between the calibrated *Hipparcos* and *Gaia* proper motions from Brandt (2018) and the best fit orbit. The sum of the  $\chi^2$  of the fits to both proper motions is very good (nearly 1, see Table 4). There are six measurements, but the unknown barycenter proper motion removes two degrees of freedom. The reflex motion of  $\beta$  Pic c with a period of  $\sim$ three years is clearly seen, as well as the long term oscillation from the  $\sim 24$  year orbit of  $\beta$  Pic b. Here the constraining power of the *Hipparcos* proper motion is visible: the *Hipparcos* proper motion is much more precise than that of *Gaia*

<sup>3</sup> `orvara` completes this million-step MCMC in roughly 4 hours on a 4 GHz AMD Ryzen desktop processor.

<sup>4</sup> The chains and input data are available by request.

**Table 1.** Posteriors of the  $\beta$  Pic system from an **orvara** MCMC analysis.

Parameter	Prior Distribution	Posteriors $\pm 1\sigma$	
Stellar mass	Uniform	$1.83 \pm 0.04 M_{\odot}$	
Parallax	$50.62 \pm 0.33$ mas ( <i>Gaia</i> DR2)	$50.58 \pm 0.47$ mas	
Barycenter Proper Motions	Uniform	$\mu_{\alpha} = 4.80 \pm 0.03$ mas yr $^{-1}$ & $\mu_{\delta} = 83.87 \pm 0.03$ mas yr $^{-1}$	
RV Zero Point	Uniform	$33 \pm 13$ m/s	
RV jitter	Log uniform over [0, 300 m/s]	$50 \pm 8$ m/s	
Parameter	Prior Distribution	Posterior on $\beta$ Pic b $\pm 1\sigma$	Posterior on $\beta$ Pic c $\pm 1\sigma$
Semi-major axis ( $a$ )	Uniform	$10.31 \pm 0.11$ A.U.	$2.75^{+0.040}_{-0.035}$ A.U.
Eccentricity	Uniform	$0.121 \pm 0.008$	${}^a 0.30^{+0.20}_{-0.16}$
Inclination	$\sin i$ (geometric)	$88.94 \pm 0.02$ degrees	$89.1 \pm 0.68$ degrees
PA of ascending node ( $\Omega$ )	Uniform	$211.95 \pm 0.030$ degrees	$211 \pm 0.25$ degrees
Mean Longitude at $t_{\text{ref}}$ ( $\lambda_{\text{ref}}$ )	Uniform	$-36.9 \pm 1.0$ degrees	$-52^{+15}_{-17}$ degrees
Planet Mass ( $M$ )	Uniform	$9.8^{+2.7}_{-2.6} M_{\text{Jup}}$	$8.3^{+1.1}_{-1.0} M_{\text{Jup}}$
Argument of Periastron ( $\omega$ )	(derived quantity)	$19.3^{+3.1}_{-3.2}$ degrees	$114.3^{+19}_{-3.0}$ degrees
Periastron Time ( $T_0$ )	(derived quantity)	$2456581^{+67}_{-70}$ BJD	$2455780^{+78}_{-58}$ BJD
Period	(derived quantity)	$8880 \pm 123$ days	$1223^{+24}_{-18}$ days
		$24.30 \pm 0.34$ years	$3.348^{+0.066}_{-0.051}$ years
<b>orvara</b> Reference Epoch ( $t_{\text{ref}}$ )	2455197.50 BJD	...	...

NOTE—Orbital elements all refer to orbit of the companion about the barycenter. The orbital parameters for  $\beta$  Pic A about each companion are identical except  $\omega_A = \omega + \pi$ . We use  $\pm$  when the posteriors are Gaussian. In the case of non-Gaussian posteriors we denote the value by  $\text{median}^{+u}_{-l}$  where  $u$  and  $l$  denote the 68.3% confidence interval about the median.

<sup>a</sup>The posterior on the eccentricity of  $\beta$  Pic c is not Gaussian. However, eccentricities below 0.1 and above 0.8 are strongly disfavored (See Figure 3).

DR2 for  $\beta$  Pic b and can exert a sizable tug on the mass and mass uncertainty of  $\beta$  Pic b.

Figures 5 and 6 show the agreement in relative separation and PA from our set of relative astrometry (Case 3 from Nielsen et al. (2020) plus the seven GRAVITY measurements on  $\beta$  Pic b and three GRAVITY measurements on  $\beta$  Pic c). Figure 7 shows the agreement between the RVs from Vandal et al. (2020) and Lagrange et al. (2020) and the best-fit orbit. The jitter parameter found by the MCMC analysis is  $50 \pm 8$  m/s. Lower masses for  $\beta$  Pic c slightly favor lower eccentricities.

We display an additional corner plot in Figure 8 that showcases select covariances between the orbital parameters of  $\beta$  Pic b and  $\beta$  Pic c. The inferred mass of each planet is relatively insensitive to the orbital parameters of the other (see the two appropriate covariances in the left hand columns of Figure 8). In particular, the mass of  $\beta$  Pic b is nearly independent of the mass of c. However, owing to the 3-body interaction between the planets, the inferred eccentricity of  $\beta$  Pic b varies slightly with the eccentricity of the inner planet,  $\beta$  Pic c. The inferred semi-major axis of  $\beta$  Pic c covaries modestly with  $\beta$  Pic b’s eccentricity as well. Despite uncertain-

ties in the eccentricity of  $\beta$  Pic c, we find that  $\beta$  Pic b and  $\beta$  Pic c are coplanar to within a half-degree at 68% confidence and coplanar to within one degree at 95% confidence.

We use our new constraints on the orbital parameters of  $\beta$  Pic b and c to predict the positions of both  $\beta$  Pic b and c over the next 2 years. In Tables 2 and 3 we show the predicted positions of  $\beta$  Pic b and c, respectively, in right-ascension and declination offsets from the star.  $\beta$  Pic c will be less than  $\sim 50$  mas from the star by May of 2021.  $\beta$  Pic c will re-emerge (once again being further than  $\sim 50$  mas from the star) in November of 2021.

### 3.2. Assessing Relative Astrometry

Table 4 shows quantitatively the goodness of the orbital fit in terms of  $\chi^2 = \sum(\text{data} - \text{model})^2/\sigma^2$  for PA, separation, RV, and the three proper motions. The reduced  $\chi^2$  for all the astrometry (which takes into account the GRAVITY covariances between separation and PA) is 1.1. A good fit should have  $\chi^2/N \approx 1$  where  $N$  is the number of degrees of freedom.

Nielsen et al. (2020) argued for a systematic offset between the SPHERE relative astrometry from Lagrange

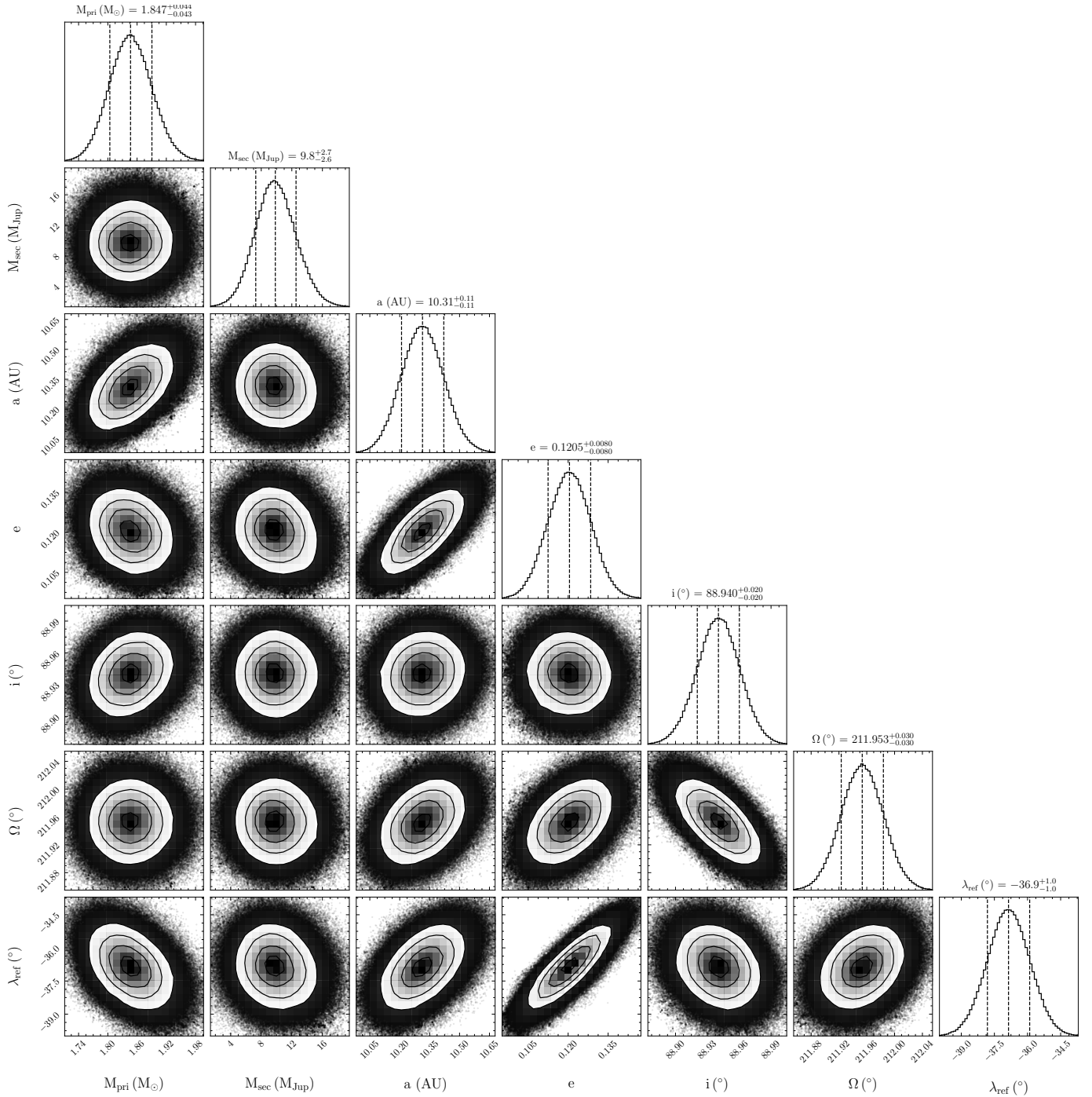


**Figure 2.** Best fit orbital elements for  $\beta$  Pic b from the *orvara* MCMC chain. Orbital elements are with respect to the star. The elements, in the same order as plotted, are: the primary mass in solar masses,  $M_{\text{pri}}$ ; the planet mass in Jupiter masses,  $M_{\text{sec}}$ ; the semi-major axis in A.U.,  $a$ ; the eccentricity,  $e$ ; the inclination in degrees,  $i$ ; the PA of the ascending node in degrees,  $\Omega$ ; and the mean longitude at the reference epoch (2455197.50 BJD) in degrees,  $\lambda_{\text{ref}}$ . The vertical-dashed lines about the center dashed lines give the 16 and 84% quantiles around the median.

et al. (2019b) and the relative astrometry from Gemini-South/GPI. Nielsen et al. (2020) investigated fitting for an offset in both separation and PA within the SPHERE data. We find corroborating evidence for an offset between the SPHERE relative astrometry and the rela-

tive astrometry from VLT/NACO, Gemini-South/NICI, Magellan/MagAO, Gemini-South/GPI, and GRAVITY. First, the SPHERE data are systematically offset in separation relative to the best-fit orbit without SPHERE data. Second, when the SPHERE data are incorporated

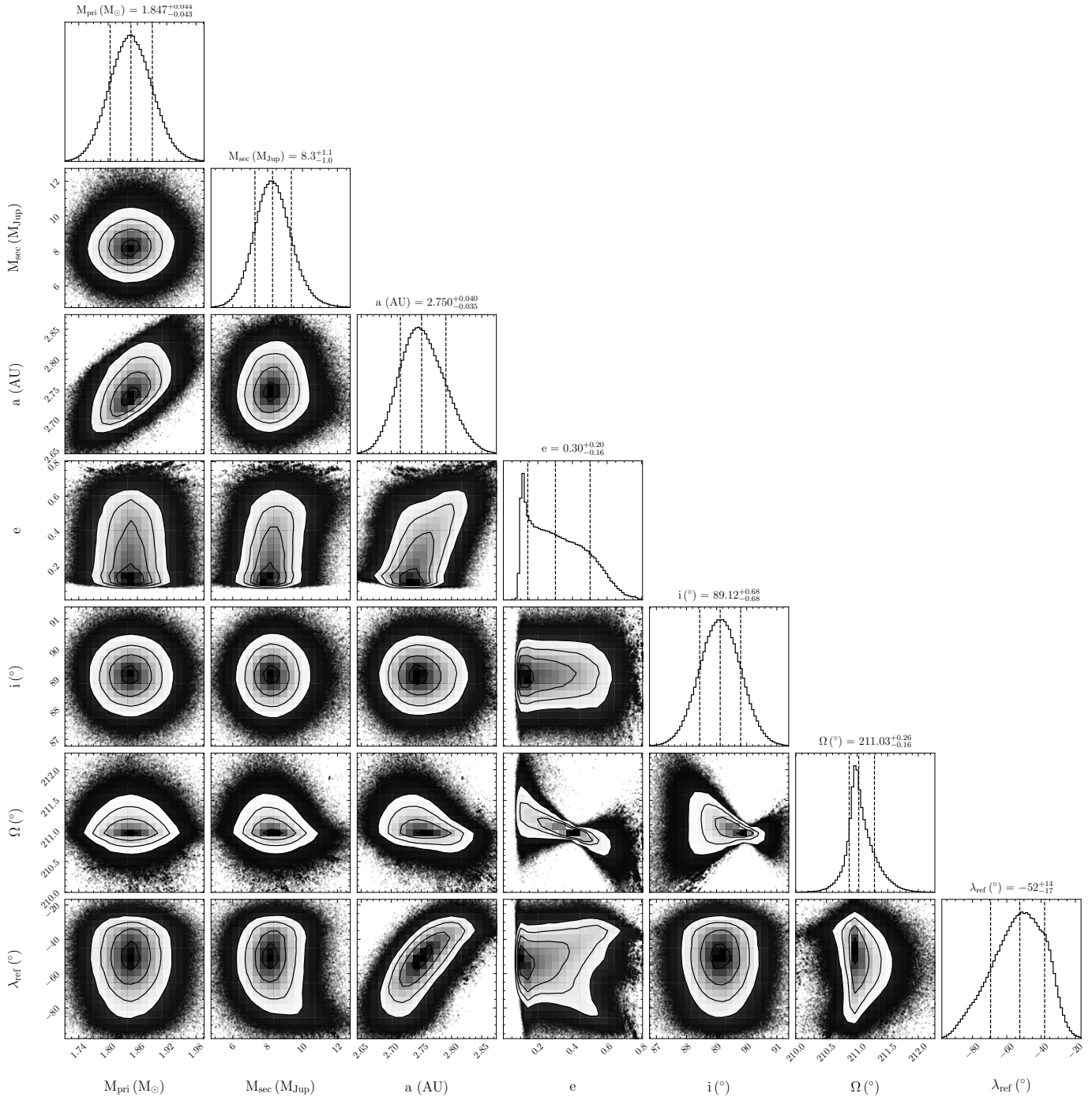


**Figure 3.** Best fit orbital elements for  $\beta$  Pic c. See Figure 2 for the description.

in a joint orbital fit, the reduced  $\chi^2$  in separation jumps from  $\approx 1$  (see Table 4) to nearly 5. These two observations suggest a systematic disagreement between the Lagrange et al. (2019b) SPHERE astrometry and the astrometry from GRAVITY and the other four instruments. The reduced  $\chi^2$  in PA stays near 1, meaning that we find that the SPHERE data primarily disagree in separation with respect to the other data sets. We conclude that one should likely include an additional

parameter in the MCMC orbital fit to account for an offset in separation or plate scale to the Lagrange et al. (2019b) relative astrometry. However, we find that including the SPHERE relative astrometry changes the best-fit inferred masses of  $\beta$  Pic b and c by less than  $0.5 M_{\text{Jup}}$ . Given the exquisite precision of GRAVITY, evidence for an offset in SPHERE from both our analyses and the analyses of Nielsen et al. (2020), we chose to

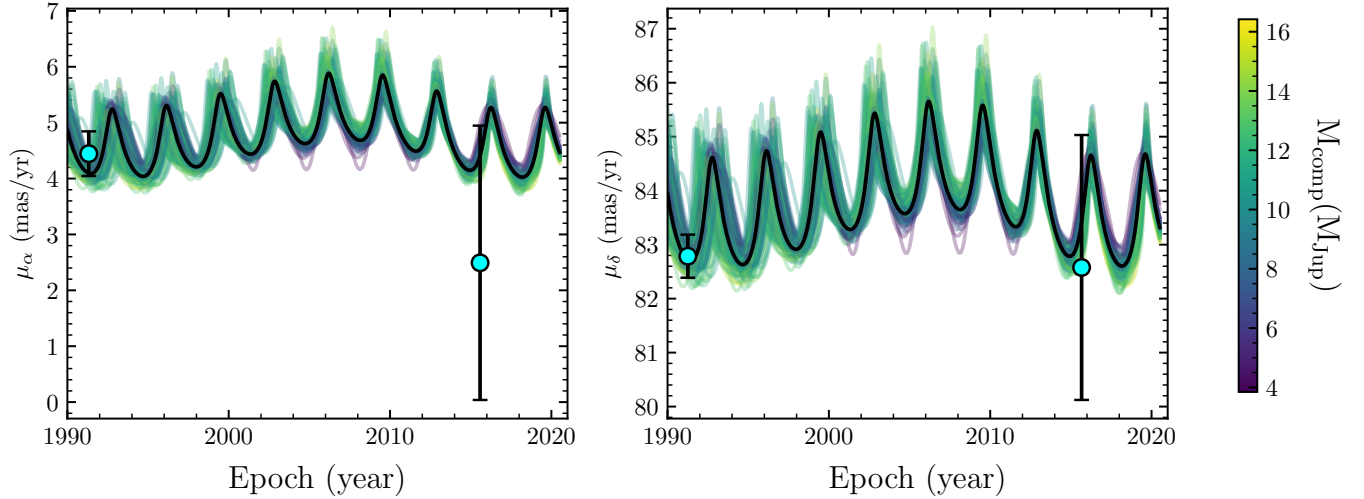


**Figure 4.** Model proper motions compared to the calibrated *Hipparcos* (dot at 1991.25) and *Gaia* proper motions (dot near 2015) from the HGCA. The *Gaia* DR2 proper motion uncertainty has been inflated by an extra factor of 2, as in Dupuy et al. (2019), to account for additional uncertainties with stars as bright as  $\beta$  Pic (see Figure 9 of Brandt 2018). The best fit orbit is shown in black. A random sampling of other orbits from the MCMC chain are shown and are color coded by the mass of  $\beta$  Pic b.

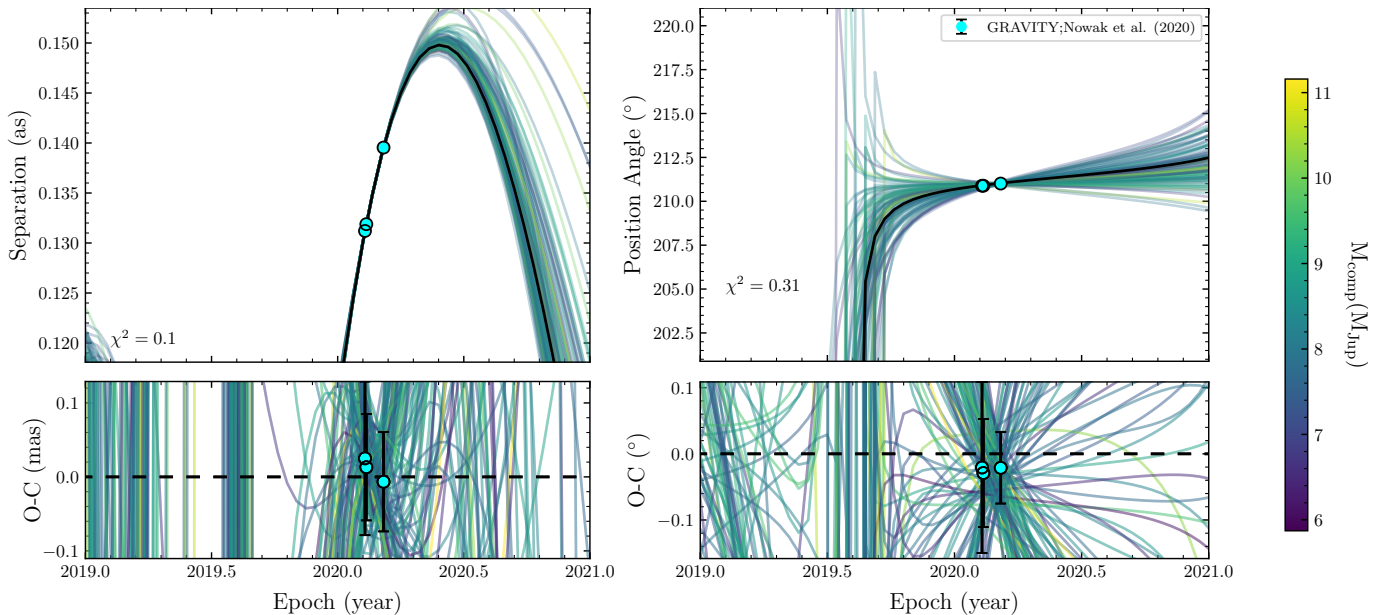


**Figure 5.** Left: relative separation of  $\beta$  Pic c. Right: PA of  $\beta$  Pic c. All three data points are from GRAVITY (Nowak et al. 2020) and are not error inflated. The best fit orbit is shown in black. A random sampling of other orbits from the MCMC chain are shown and are color coded by the mass of  $\beta$  Pic c.

exclude the Lagrange et al. (2019b) relative astrometry from our final orbital fit.

In Figure 5, the  $\chi^2$  of the  $\beta$  Pic c fit to the relative astrometry is much less than 1 because the relative astrometry is effectively overfit: the RVs primarily constrain the mass, phase, and semimajor axis of  $\beta$  Pic c while the four remaining orbital parameters have substantial freedom to fit the three relative astrometry points (6 co-

ordinates). By contrast,  $\beta$  Pic b is overconstrained by the data and the reduced  $\chi^2$  of the fit is near 1 ( $\chi^2 \approx 50$  for 44 data points). The right-hand side of the bottom-most panel for both separation and PA in Figure 6 show the GRAVITY points in cyan for  $\beta$  Pic b. GRAVITY points near the same epoch (in both PA and separation) disagree by  $\lesssim 1\sigma$  after error-inflation. Without error inflation, GRAVITY observations near the same

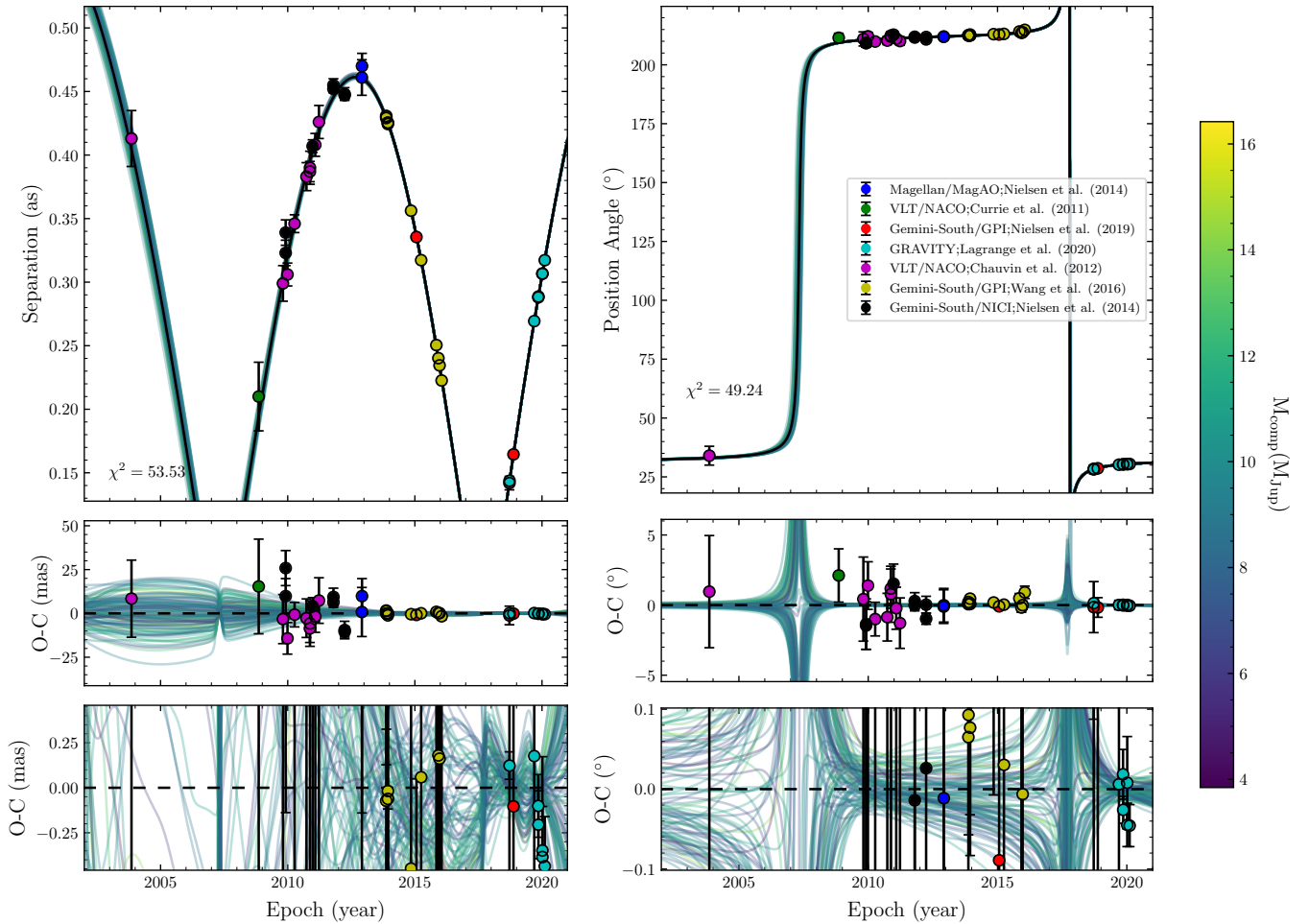


**Figure 6.** Left: relative separation of  $\beta$  Pic b. Right: PA of  $\beta$  Pic b. The GRAVITY errors have been inflated by a factor of two to make the reduced  $\chi^2$  of the fit acceptable. A random sampling of orbits from other MCMC steps are shown and are color coded by the mass of  $\beta$  Pic b. The best fit orbit is shown in black.

epoch disagree by  $\sim 2\sigma$  and the reduced  $\chi^2$  in PA of the best fit jumps to nearly 3 for  $\beta$  Pic b.

The three GRAVITY measurements of  $\beta$  Pic c do not have  $\chi^2$  or agreement issues. We leave the errors on  $\beta$  Pic c as they are in Nowak et al. (2020). However, inflating the errors by a factor of 2 on  $\beta$  Pic c does not significantly change our results: the resulting posteriors and errors are identical except for the errors on inclination, which are doubled.

### 3.3. *N*-body Simulations

We expect the orbital parameters of  $\beta$  Pic b and c to vary over time due to the mutual influence between these two massive planets. The evolution of the eccentricity and orbit of  $\beta$  Pic b depends heavily on the eccentricity of  $\beta$  Pic c, which is poorly constrained. In Figure 9, we show the evolution of the  $\beta$  Pic system over 0.1 million years (Myr), integrated forward using the ias15 integrator of REBOUND (Rein & Liu 2012; Rein & Spiegel 2015), assuming the median orbital param-

eters presented in Table 1 for each planet. We vary the eccentricity of  $\beta$  Pic c within the posterior constraints. The grey shaded region shows how the eccentricity of  $\beta$  Pic c and  $\beta$  Pic b could evolve over the next  $10^5$  years. The two planets exchange eccentricity with a period of  $\sim 50,000$  years. We found numerically that the system is stable and the periodic variability in Figure 9 repeats for at least the next 10 Myr.

## 4. DISCUSSION

Our mass measurements for  $\beta$  Pic b and c agree within  $1\sigma$  compared to previous work by Snellen & Brown (2018), Dupuy et al. (2019), Nielsen et al. (2020), and Vandal et al. (2020). Our analysis is the first to incorporate the new GRAVITY measurements with uninformative priors while obtaining masses in the expected expected range. Our error bars on the mass of  $\beta$  Pic b are larger than all but Dupuy et al. (2019) because, like that work, we adopt the inflated errors on the *Hipparcos* proper motions as recommended by Brandt

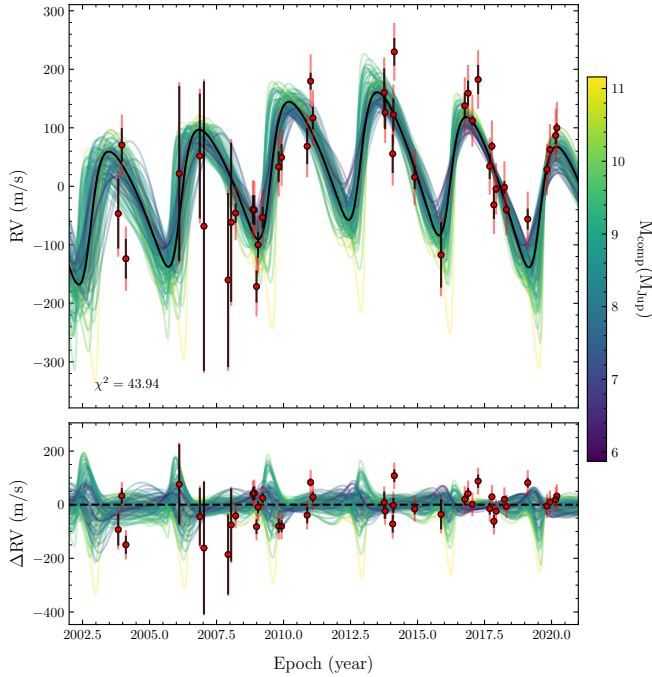


**Figure 7.** The best fit orbit (black) agrees well with the observed  $\beta$  Pic pulsation-corrected RVs.  $\beta$  Pic c has an eccentricity of  $e = 0.28$  in the best fit orbit while b has  $e = 0.125$ . Top panel: The observed RVs overplot with the best fit orbit and a random sampling of other orbits from the MCMC chain. Bottom panel: The RV residuals with respect to the best fit orbit. Both panels: The random sampling of other orbits from the MCMC chain are color coded by the mass of  $\beta$  Pic c. RVs are from Vandal et al. (2020) with the most recent 5 points from Lagrange et al. (2020). The black error bars give the observed errors reported by Vandal et al. (2020) and Lagrange et al. (2020). The red error bars include the best fit jitter of  $\sim 50$  m/s added in quadrature to the observed errors.

(2018). We were unable to reproduce the  $\approx 3 M_{\text{Jup}}$  and  $\approx 5 M_{\text{Jup}}$  (when using a uniform prior) mass estimates from Nowak et al. (2020) and Lagrange et al. (2020). Using their slightly different data set, we find  $9.1^{+2.0}_{-1.8} M_{\text{Jup}}$  for  $\beta$  Pic b and  $9.1^{+0.9}_{-0.8} M_{\text{Jup}}$  for  $\beta$  Pic c.

We corroborate the findings by Nielsen et al. (2020) and Nowak et al. (2020) that  $\beta$  Pic c and  $\beta$  Pic b are coplanar. Nowak et al. (2020) found inclinations for  $\beta$  Pic b and c of  $88.99 \pm 0.01$  degrees and  $89.17 \pm 0.50$  degrees, respectively, with a Gaussian prior on the mass of  $\beta$  Pic b. We confirm these inclinations without an informative prior. We find  $88.94 \pm 0.02$  degrees and  $89.1 \pm 0.7$  degrees. Our uncertainty in the inclination of  $\beta$  Pic b is twice as large due to the exclusion of the Lagrange et al. (2019b) relative astrometry.

$\beta$  Pic is surrounded by an extended debris disc and an inner disc that is slightly misaligned with respect to the primary (Smith & Terrile 1984; Heap et al. 2000). The

**Table 2.** Predicted positions of  $\beta$  Pic b.

MJD	$\alpha$	$\sigma_\alpha$	$\delta$	$\sigma_\delta$
59163	203.7	0.46	339.5	0.3
59187.138	207.2	0.5	344.9	0.32
59211.276	210.7	0.55	350.3	0.35
59235.414	214.1	0.6	355.5	0.38
59259.552	217.4	0.65	360.7	0.41
59283.69	220.7	0.7	365.8	0.44
59307.828	223.9	0.76	370.8	0.47
59331.966	227.1	0.82	375.6	0.51
59356.103	230.2	0.88	380.4	0.55
59380.241	233.3	0.95	385.1	0.58
59404.379	236	1	389.7	0.62
59428.517	239	1.1	394.3	0.67
59452.655	242	1.2	398.7	0.71
59476.793	245	1.2	403	0.76
59500.931	248	1.3	407.2	0.8
59525.069	250	1.4	411.3	0.85
59549.207	253	1.5	415.4	0.9
59573.345	256	1.6	419.3	0.96
59597.483	258	1.7	423	1
59621.621	261	1.8	427	1.1
59645.759	263	1.9	430	1.1
59669.897	266	2	434	1.2
59694.034	268	2.1	437	1.2
59718.172	270	2.2	441	1.3
59742.31	272	2.3	444	1.4
59766.448	274	2.4	447	1.4
59790.586	276	2.5	450	1.5
59814.724	278	2.6	453	1.6
59838.862	280	2.7	456	1.7
59863	282	2.9	459	1.7

NOTE—A non-rounded, machine readable version of this table and a table with 2-day cadence are available as supplementary data online (or with the source TeX files if viewing this on ArXiv). The right-ascension ( $\alpha$ ) and declination ( $\delta$ ) offsets from the star and their errors are given in milli-arcseconds.

extended debris disc around  $\beta$  Pic is inclined at  $90.0 \pm 0.1$  degrees (Ahmic et al. 2009; Kraus et al. 2020).  $\beta$  Pic b is thus misaligned by  $1.06 \pm 0.11$  degrees with respect to the debris disc. Our inferred inclination for  $\beta$  Pic c slightly favors misalignment but does not exclude alignment.

Nowak et al. (2020) found that the  $\beta$  Pic system exhibited an oscillating eccentricity for both bodies over a

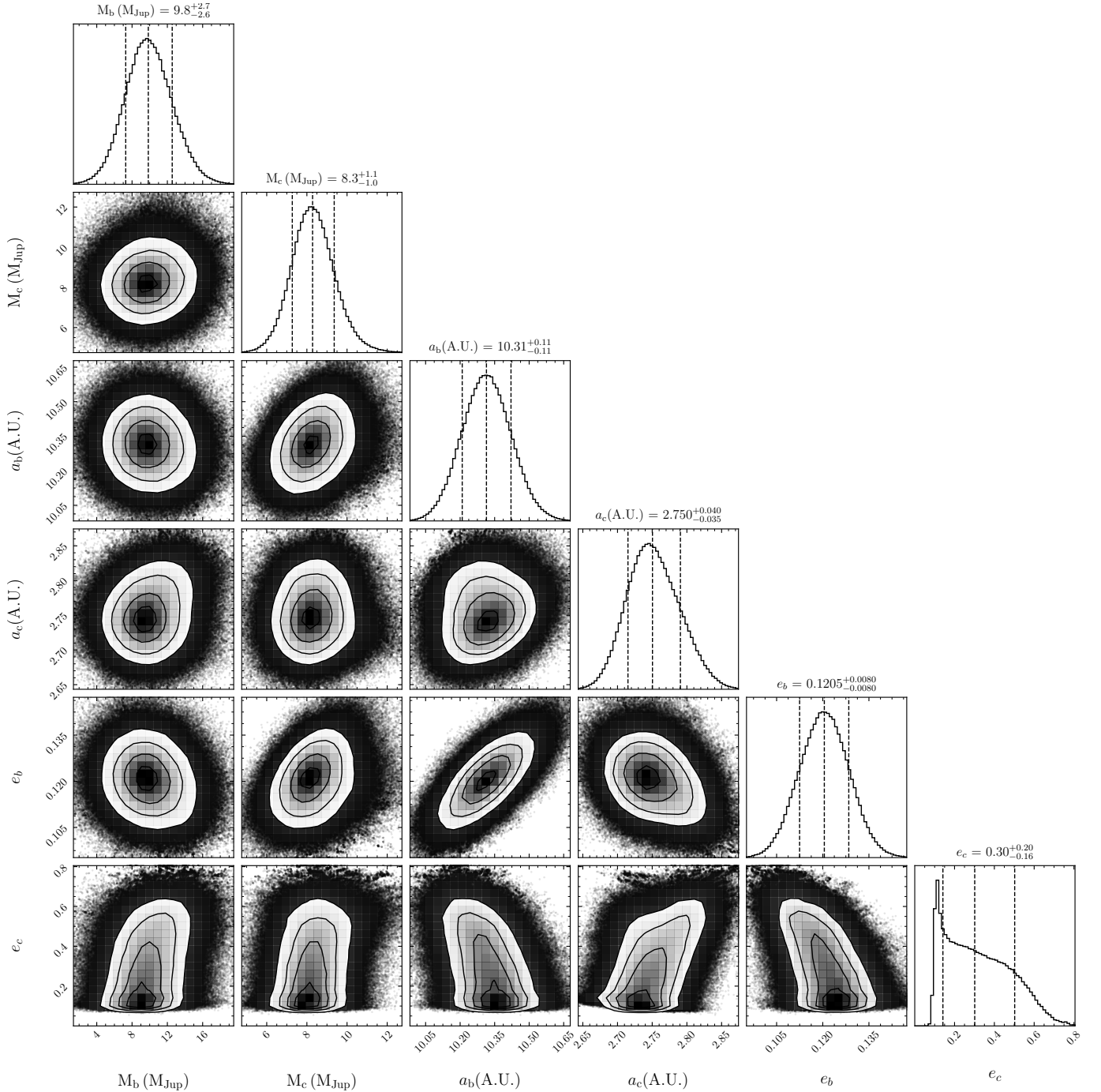


**Figure 8.** The masses of  $\beta$  Pic c and  $\beta$  Pic b are mostly unaffected by the eccentricity of  $\beta$  Pic c. However, the inferred eccentricity of b is moderately sensitive to the eccentricity of  $\beta$  Pic c due to 3-body interactions. We showcase here a selection of best fit orbital elements for both  $\beta$  Pic c and  $\beta$  Pic b along with the covariances between them. These are: The masses of  $\beta$  Pic b and c in Jupiter masses,  $M_b$  and  $M_c$ ; the semi-major axes of both planets in A.U.,  $a_b$  and  $a_c$ ; and their eccentricities,  $e_b$  and  $e_c$ .

timescale of  $\approx 5 \times 10^4$  years using their orbital parameter posteriors. We find variations in eccentricity over a similar timescale and confirmed numerically with REBOUND that the system is stable for at least the next 10 Myr. We find that it is moderately likely to observe the cur-

rent eccentricity of the system amidst all the possible eccentricities over a 10 million year timespan.

The first observational evidence that  $\beta$  Pic b has a significant, nonzero eccentricity was presented by Dupuy et al. (2019). They discussed the implications of an ec-

**Table 3.** Predicted positions of  $\beta$  Pic c.

MJD	$\alpha$	$\sigma_\alpha$	$\delta$	$\sigma_\delta$
59163	-60	7.5	-107	4.6
59187.138	-55	9.3	-100	5.7
59211.276	-50	11	-93	6.9
59235.414	-40	13	-84	8.1
59259.552	-40	16	-76	9.5
59283.69	-30	18	-70	11
59307.828	-30	20	-60	12
59331.966	-20	23	-50	14
59356.103	-10	25	-40	16
59380.241	0	28	-30	17
59404.379	0	30	-10	18
59428.517	10	32	0	20
59452.655	20	33	10	21
59476.793	20	34	20	22
59500.931	30	35	20	22
59525.069	40	36	30	22
59549.207	50	35	40	22
59573.345	50	35	50	22
59597.483	60	33	50	21
59621.621	60	31	60	20
59645.759	60	29	60	19
59669.897	70	26	70	17
59694.034	70	23	70	15
59718.172	70	20	70	13
59742.31	60	17	70	11
59766.448	60	16	71	9.8
59790.586	50	16	68	9.4
59814.724	50	18	60	10
59838.862	40	21	50	12
59863	30	24	40	14

NOTE—A non-rounded, machine readable version of this table and a table with 2-day cadence are available as supplementary data online (or with the source TeX files if viewing this on ArXiv). The right-ascension ( $\alpha$ ) and declination ( $\delta$ ) offsets from the star and their errors are given in milli-arcseconds.

centricity as high as  $\approx 0.2$  in the context of both single- and multi-planet scenarios; at the time  $\beta$  Pic c was not known. The scenario in which  $\beta$  Pic b formed on a circular orbit but gained eccentricity from interactions with the disk and migrated inward to its current loca-

**Table 4.** The goodness of the *orvara* orbital fit to the various data in the  $\beta$  Pic system.

Data	Number of points ( $N$ )	$\chi^2$
Separation	44	54.5
PA	44	49.6
All Astrometry	88	<sup>a</sup> 97.9
RV	41	43.9
Hipparcos $\mu$ (HGCA)	2	0.25
Gaia $\mu$ (HGCA)	2	0.75
HGCA long baseline $\mu$	2	0.001

NOTE—The  $\chi^2$  quoted here include both companions and are for the maximum likelihood orbits. The  $\chi^2$  for  $\mu$  includes both  $\mu_\delta$  and  $\mu_\alpha$ .

<sup>a</sup>This  $\chi^2$  of 97.9 is slightly less than the sum of the  $\chi^2$  in PA and separation because of the covariance between PA and separation in the GRAVITY observations.

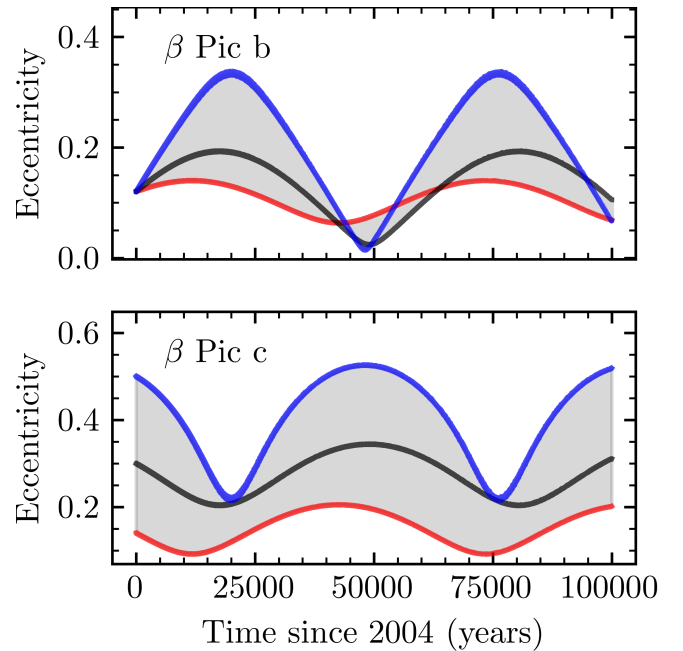


**Figure 9.** Top panel: the eccentricity evolution of  $\beta$  Pic b computed using REBOUND’s *ias15* integrator (Rein & Spiegel 2015) for the median (black, 0.30) and 68.3% confident bounds on the eccentricity of  $\beta$  Pic c from Table 1 (0.14 is red and 0.50 is blue). Bottom panel: the eccentricity evolution of  $\beta$  Pic c for its median (black) and 68.3% confident eccentricities. The parameter space spanned by the 68.3% confident range of eccentricities is shaded grey. The two planets exchange eccentricity over a  $\sim 50,000$  year cycle.

tion, with no influence from  $\beta$  Pic c, is still plausible. Such a pathway is available to any sufficiently massive

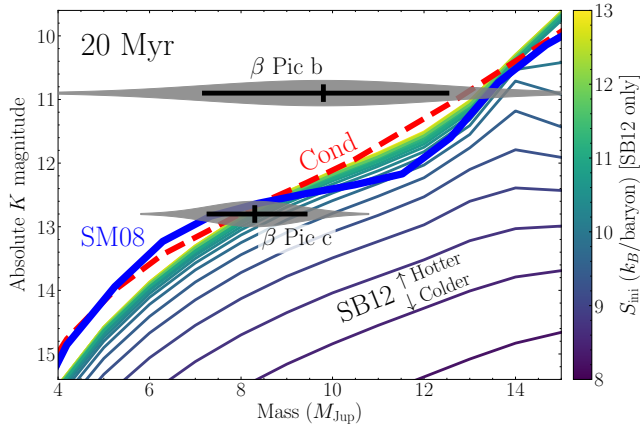


**Figure 10.** Comparison of dynamical mass measurements (gray shaded regions) and observed  $K$ -band magnitudes (Nowak et al. 2020) with Cond (Baraffe et al. 2003), SM08 (Saumon & Marley 2008), and SB12 (Spiegel & Burrows 2012) models, all at an age of 20 Myr (Binks & Jeffries 2014; Mamajek & Bell 2014; Miret-Roig et al. 2020). The SM08 and SB12 models both use hybrid cloud prescriptions and adopt Solar metallicity. The SB12 models also vary (and are color-coded by) their initial entropy. The black lines show  $1\sigma$  values, while gray shaded regions show the probability density. Our dynamical mass for  $\beta$  Pic c is consistent with all three models assuming a hot start, and rules out a very cold start. Our dynamical mass for  $\beta$  Pic b is  $\sim 1\sigma$  below the prediction of the hot start models.

planet. Given that we find that  $\beta$  Pic c is also massive ( $8.3_{-1.0}^{+1.1} M_{\text{Jup}}$ ), it may have also opened a gap in the disk, migrating inward and acquiring eccentricity from gravitational interactions with  $\beta$  Pic b and the disk. Indeed, with two such massive planets in close proximity it is natural to expect that both should have significantly nonzero eccentricities by a system age of  $\approx 20$  Myr.

Our masses follow from uniform priors, allowing us to independently assess the agreement of the dynamical masses with model predictions. To simplify our model comparisons, we assume an age of 20 Myr for the system, compatible with all available age determinations for the  $\beta$  Pic moving group (Binks & Jeffries 2014; Mamajek & Bell 2014; Miret-Roig et al. 2020). We examine the hot-start Cond (Baraffe et al. 2003) models, the Saumon & Marley (2008) models with a hybrid cloud treatment (which we denote as SM08), and the warm-start Spiegel & Burrows (2012) models (SB12) with hybrid clouds and solar metallicity but a range of initial entropies. We perform our comparisons in the  $K$  band, as this is the only measurement available for  $\beta$  Pic c (Nowak et al. 2020). We convert luminosities to  $K$ -band magnitudes for the SM08 models using Cond colors at the SM08 effective temperatures.

Figure 10 shows our results. We find that our dynamical mass measurement for  $\beta$  Pic c is consistent with all models except those with low initial entropies ( $\lesssim 10 k_{\text{B}}/\text{baryon}$ ). Our dynamical mass for  $\beta$  Pic b is roughly  $1\sigma$  below the predictions of hot-start models, and rules out cold starts. Similarly to previous work (Dupuy et al. 2019; Vandal et al. 2020), none of the disagreements with models are significant beyond  $\sim 1\sigma$ , and the precisions of the dynamical masses are insufficient to distinguish between most of the models shown. Stronger tests of models will require significantly better precision, especially for  $\beta$  Pic b.

As Figure 10 shows, reaching  $0.1\text{--}0.5 M_{\text{Jup}}$  levels of precision on the mass of  $\beta$  Pic b is crucial to accurately discern between evolutionary models. The best prospect for improving the mass of  $\beta$  Pic b is long term RV monitoring over the next decade. Even drastically improved absolute astrometry (e.g., *Gaia* DR4) will only provide a modest improvement to the mass measurement of  $\beta$  Pic b. If we assume optimistically that *Gaia* at the end of its mission will achieve the same precision on the  $G = 3.7$  mag  $\beta$  Pic A as it has on  $G \approx 6$  mag stars (the brightest for which the mission was originally designed), then it would achieve a factor of  $\sim 100$  improvement on the proper motion of  $\beta$  Pic A.<sup>5</sup> The uncertainty on the mass of  $\beta$  Pic b would shrink by 35%, to  $\pm 1.7 M_{\text{Jup}}$ , if the proper motion precision is improved by a factor of 100—using the same MCMC analysis as presented here with otherwise the same data. Assuming more conservatively that *Gaia* reaches only a factor of 10 better precision on the proper motion of  $\beta$  Pic, the uncertainty on the mass of  $\beta$  Pic b improves by 25%.

## 5. CONCLUSIONS

In this paper we have derived masses and orbits of both planets in the  $\beta$  Pictoris system with uninformative priors. We validated our approach against synthetic data from a full  $N$ -body integration. Our masses and orbital parameters are derived from two decades of observational data. The data show clear evidence of the gravitational perturbations of  $\beta$  Pic c ( $P = 3.348_{-0.05}^{+0.07}$  yr) on the orbit of  $\beta$  Pic b relative to A ( $P = 24.30 \pm 0.34$  yr). The resulting model-independent masses allow us to compare the observed properties of  $\beta$  Pic b and c with predictions from models of the formation and evolution of giant planets. We summarize our main results below.

1. The eccentricity and mean longitude of  $\beta$  Pic c are poorly constrained because there are only three relative astrometric observations, and these are

<sup>5</sup> <https://www.cosmos.esa.int/web/gaia/science-performance>

closely spaced in time. There is a mild covariance between the eccentricity of  $\beta$  Pic b and c owing to the three-body dynamics in the system. Additional GRAVITY relative astrometry on  $\beta$  Pic c will help constrain the eccentricity of  $\beta$  Pic b and especially  $\beta$  Pic c.

2. We find a mass of  $9.8_{-2.6}^{+2.7} M_{\text{Jup}}$  for  $\beta$  Pic b and  $8.3_{-1.0}^{+1.1} M_{\text{Jup}}$  for  $\beta$  Pic c with uninformative priors all orbital parameters. The mass constraint on  $\beta$  Pic c is superior due to the RVs covering many orbital periods and due to the impact of  $\beta$  Pic c on the relative astrometry of  $\beta$  Pic b.
3.  $\beta$  Pic b and  $\beta$  Pic c are both consistent with Spiegel & Burrows (2012) warm-start models with initial entropies of at least  $10 k_{\text{B}}$ /baryon. They are also both consistent with a 20 Myr age under the hot-start COND evolutionary tracks (Baraffe et al. 2003) and the Saumon & Marley (2008) models using a hybrid cloud model. In all cases, consistency with models would favor a mass for  $\beta$  Pic b that is  $\sim 1\sigma$  higher than our dynamical measurement.
4. The mass constraint on  $\beta$  Pic b needs to be improved by a factor of  $\sim 3$ – $5$  in order to more reliably constrain its age or formation conditions. Long-term RV monitoring over the coming years or decade is needed for better mass constraints on  $\beta$  Pic b. An improved proper motion from a future *Gaia* data release will offer up to a 35% better constraint on the mass of  $\beta$  Pic b (assuming *Gaia* reaches a better precision on the brightest stars).

The new set of GRAVITY astrometry appeared to draw tension between dynamical and spectral mass constraints on  $\beta$  Pic b. Our analysis and implementation

of three body interactions dissolves this tension and results in masses for  $\beta$  Pic b and  $\beta$  Pic c that are consistent with warm and hot start models. As well, the system is dynamically interesting – with eccentricities of both planets varying by  $\sim 50\%$  over  $10^4$ – $10^5$  year timescales. The precision on the masses and eccentricities of  $\beta$  Pic b will improve with continued astrometric and RV monitoring. The planets around  $\beta$  Pic A will continue to provide some of the best tests of super-Jovian planet formation and evolution.

*Software:* `astropy` (Astropy Collaboration et al. 2013; Price-Whelan et al. 2018), `scipy` (Virtanen et al. 2020), `numpy` (Oliphant 2006; van der Walt et al. 2011), `pandas` (Wes McKinney 2010; pandas development team 2020), `orvara` (Brandt et al. 2020, submitted), `htof` (Brandt & Michalik 2020; Brandt et al. 2020, submitted), `REBOUND` (Rein & Liu 2012), `corner` (Foreman-Mackey 2016), `Jupyter`

#### ACKNOWLEDGMENTS

G. M. Brandt is supported by the National Science Foundation (NSF) Graduate Research Fellowship under grant no. 1650114.

We thank Kaitlin Kratter for fruitful discussions and comments.

This work made use of the `REBOUND` code which is freely available at <http://github.com/hannorein/rebound>.

This work made use of the `orvara` code. The exact version we used is available via the git hash `51757c58dc78db406a39503b509a929253b9`.

This work made use of the `htof` code. We used version `0.3.1`.

#### REFERENCES

- Ahmic, M., Croll, B., & Artymowicz, P. 2009, *ApJ*, 705, 529, doi: [10.1088/0004-637X/705/1/529](https://doi.org/10.1088/0004-637X/705/1/529)
- Astropy Collaboration, Robitaille, T. P., Tollerud, E. J., et al. 2013, *A&A*, 558, A33, doi: [10.1051/0004-6361/201322068](https://doi.org/10.1051/0004-6361/201322068)
- Baraffe, I., Chabrier, G., Barman, T. S., Allard, F., & Hauschildt, P. H. 2003, *A&A*, 402, 701, doi: [10.1051/0004-6361:20030252](https://doi.org/10.1051/0004-6361:20030252)
- Barrado y Navascués, D., Stauffer, J. R., Song, I., & Caillault, J. P. 1999, *ApJL*, 520, L123, doi: [10.1086/312162](https://doi.org/10.1086/312162)
- Bell, C. P. M., Mamajek, E. E., & Naylor, T. 2015, *MNRAS*, 454, 593, doi: [10.1093/mnras/stv1981](https://doi.org/10.1093/mnras/stv1981)
- Binks, A. S., & Jeffries, R. D. 2014, *MNRAS*, 438, L11, doi: [10.1093/mnrasl/slt141](https://doi.org/10.1093/mnrasl/slt141)
- Bonnefoy, M., Lagrange, A. M., Boccaletti, A., et al. 2011, *A&A*, 528, L15, doi: [10.1051/0004-6361/201016224](https://doi.org/10.1051/0004-6361/201016224)
- Bonnefoy, M., Boccaletti, A., Lagrange, A. M., et al. 2013, *A&A*, 555, A107, doi: [10.1051/0004-6361/201220838](https://doi.org/10.1051/0004-6361/201220838)
- Brandt, G. M., Brandt, T. D., D., M., et al. 2020, submitted, *AJ*
- Brandt, G. M., & Michalik, D. 2020, `gmbrandt/HTOF`: Paper submission release, zenodo, 0.3.0, Zenodo, doi: [10.5281/zenodo.4104384](https://doi.org/10.5281/zenodo.4104384)
- Brandt, T. D. 2018, *The Astrophysical Journal Supplement Series*, 239, 31, doi: [10.3847/1538-4365/aaec06](https://doi.org/10.3847/1538-4365/aaec06)

- Brandt, T. D., Dupuy, T. J., Li, Y., et al. 2020, submitted, ApJ
- Chauvin, G., Lagrange, A. M., Beust, H., et al. 2012, A&A, 542, A41, doi: [10.1051/0004-6361/201118346](https://doi.org/10.1051/0004-6361/201118346)
- Chilcote, J., Barman, T., Fitzgerald, M. P., et al. 2015, ApJL, 798, L3, doi: [10.1088/2041-8205/798/1/L3](https://doi.org/10.1088/2041-8205/798/1/L3)
- Chilcote, J., Pueyo, L., De Rosa, R. J., et al. 2017, AJ, 153, 182, doi: [10.3847/1538-3881/aa63e9](https://doi.org/10.3847/1538-3881/aa63e9)
- Currie, T., Thalmann, C., Matsumura, S., et al. 2011, ApJL, 736, L33, doi: [10.1088/2041-8205/736/2/L33](https://doi.org/10.1088/2041-8205/736/2/L33)
- Currie, T., Thalmann, C., Matsumura, S., et al. 2011, The Astrophysical Journal, 736, L33, doi: [10.1088/2041-8205/736/2/L33](https://doi.org/10.1088/2041-8205/736/2/L33)
- Dupuy, T. J., Brandt, T. D., Kratter, K. M., & Bowler, B. P. 2019, ApJL, 871, L4, doi: [10.3847/2041-8213/aafb31](https://doi.org/10.3847/2041-8213/aafb31)
- ESA, ed. 1997, The HIPPARCOS and TYCHO catalogues. Astrometric and photometric star catalogues derived from the ESA HIPPARCOS Space Astrometry Mission, ESA Special Publication
- Foreman-Mackey, D. 2016, The Journal of Open Source Software, 1, 24, doi: [10.21105/joss.00024](https://doi.org/10.21105/joss.00024)
- Foreman-Mackey, D., Hogg, D. W., Lang, D., & Goodman, J. 2013, PASP, 125, 306, doi: [10.1086/670067](https://doi.org/10.1086/670067)
- Fortney, J. J., Marley, M. S., Saumon, D., & Lodders, K. 2008, ApJ, 683, 1104, doi: [10.1086/589942](https://doi.org/10.1086/589942)
- Gaia Collaboration, Prusti, T., de Bruijne, J. H. J., et al. 2016, A&A, 595, A1, doi: [10.1051/0004-6361/201629272](https://doi.org/10.1051/0004-6361/201629272)
- Gravity Collaboration, Nowak, M., Lacour, S., et al. 2020, A&A, 633, A110, doi: [10.1051/0004-6361/201936898](https://doi.org/10.1051/0004-6361/201936898)
- Heap, S. R., Lindler, D. J., Lanz, T. M., et al. 2000, The Astrophysical Journal, 539, 435, doi: [10.1086/309188](https://doi.org/10.1086/309188)
- Kraus, S., Le Bouquin, J.-B., Kreplin, A. e., et al. 2020, ApJL, 897, L8, doi: [10.3847/2041-8213/ab9d27](https://doi.org/10.3847/2041-8213/ab9d27)
- Lagrange, A. M., Bonnefoy, M., Chauvin, G., et al. 2010, Science, 329, 57, doi: [10.1126/science.1187187](https://doi.org/10.1126/science.1187187)
- Lagrange, A. M., Meunier, N., Rubini, P., et al. 2019a, Nature Astronomy, 421, doi: [10.1038/s41550-019-0857-1](https://doi.org/10.1038/s41550-019-0857-1)
- Lagrange, A. M., Boccaletti, A., Langlois, M., et al. 2019b, A&A, 621, L8, doi: [10.1051/0004-6361/201834302](https://doi.org/10.1051/0004-6361/201834302)
- Lagrange, A. M., Rubini, P., Nowak, M., et al. 2020, A&A, 642, A18, doi: [10.1051/0004-6361/202038823](https://doi.org/10.1051/0004-6361/202038823)
- Lindgren, L., Hernandez, J., Bombrun, A., et al. 2018, arxiv. <https://arxiv.org/abs/1804.09366>
- Males, J. R., Close, L. M., Morzinski, K. M., et al. 2014, ApJ, 786, 32, doi: [10.1088/0004-637X/786/1/32](https://doi.org/10.1088/0004-637X/786/1/32)
- Mamajek, E. E., & Bell, C. P. M. 2014, MNRAS, 445, 2169, doi: [10.1093/mnras/stu1894](https://doi.org/10.1093/mnras/stu1894)
- Marleau, G. D., & Cumming, A. 2014, MNRAS, 437, 1378, doi: [10.1093/mnras/stt1967](https://doi.org/10.1093/mnras/stt1967)
- Marley, M. S., Fortney, J. J., Hubickyj, O., Bodenheimer, P., & Lissauer, J. J. 2007, ApJ, 655, 541, doi: [10.1086/509759](https://doi.org/10.1086/509759)
- Miret-Roig, N., Galli, P. A. B., Brandner, W., et al. 2020, A&A, 642, A179, doi: [10.1051/0004-6361/202038765](https://doi.org/10.1051/0004-6361/202038765)
- Nielsen, E. L., Liu, M. C., Wahhaj, Z., et al. 2014, The Astrophysical Journal, 794, 158, doi: [10.1088/0004-637x/794/2/158](https://doi.org/10.1088/0004-637x/794/2/158)
- Nielsen, E. L., De Rosa, R. J., Wang, J. J., et al. 2020, AJ, 159, 71, doi: [10.3847/1538-3881/ab5b92](https://doi.org/10.3847/1538-3881/ab5b92)
- Nowak, M., Lacour, S., Lagrange, A.-M., et al. 2020, A&A, 642, L2, doi: [10.1051/0004-6361/202039039](https://doi.org/10.1051/0004-6361/202039039)
- Oliphant, T. 2006, NumPy: A guide to NumPy, USA: Trelgol Publishing. <http://www.numpy.org/>
- pandas development team, T. 2020, pandas-dev/pandas: Pandas, 1.0.5, Zenodo, doi: [10.5281/zenodo.3509134](https://doi.org/10.5281/zenodo.3509134)
- Price-Whelan, A. M., Sipőcz, B. M., Günther, H. M., et al. 2018, AJ, 156, 123, doi: [10.3847/1538-3881/aabc4f](https://doi.org/10.3847/1538-3881/aabc4f)
- Quanz, S. P., Meyer, M. R., Kenworthy, M. A., et al. 2010, ApJL, 722, L49, doi: [10.1088/2041-8205/722/1/L49](https://doi.org/10.1088/2041-8205/722/1/L49)
- Rein, H., & Liu, S. F. 2012, A&A, 537, A128, doi: [10.1051/0004-6361/201118085](https://doi.org/10.1051/0004-6361/201118085)
- Rein, H., & Spiegel, D. S. 2015, MNRAS, 446, 1424, doi: [10.1093/mnras/stu2164](https://doi.org/10.1093/mnras/stu2164)
- Saumon, D., & Marley, M. S. 2008, ApJ, 689, 1327, doi: [10.1086/592734](https://doi.org/10.1086/592734)
- Shkolnik, E. L., Anglada-Escudé, G., Liu, M. C., et al. 2012, ApJ, 758, 56, doi: [10.1088/0004-637X/758/1/56](https://doi.org/10.1088/0004-637X/758/1/56)
- Smith, B. A., & Terrile, R. J. 1984, Science, 226, 1421, doi: [10.1126/science.226.4681.1421](https://doi.org/10.1126/science.226.4681.1421)
- Snellen, I. A. G., Brandl, B. R., de Kok, R. J., et al. 2014, Nature, 509, 63, doi: [10.1038/nature13253](https://doi.org/10.1038/nature13253)
- Snellen, I. A. G., & Brown, A. G. A. 2018, Nature Astronomy, 2, 883, doi: [10.1038/s41550-018-0561-6](https://doi.org/10.1038/s41550-018-0561-6)
- Spiegel, D. S., & Burrows, A. 2012, ApJ, 745, 174, doi: [10.1088/0004-637X/745/2/174](https://doi.org/10.1088/0004-637X/745/2/174)
- van der Walt, S., Colbert, S. C., & Varoquaux, G. 2011, Computing in Science and Engineering, 13, 22, doi: [10.1109/MCSE.2011.37](https://doi.org/10.1109/MCSE.2011.37)
- van Leeuwen, F. 2007, A&A, 474, 653, doi: [10.1051/0004-6361:20078357](https://doi.org/10.1051/0004-6361:20078357)
- Vandal, T., Rameau, J., & Doyon, R. 2020, arXiv e-prints, arXiv:2009.09276. <https://arxiv.org/abs/2009.09276>
- Virtanen, P., Gommers, R., Oliphant, T. E., et al. 2020, Nature Methods, 17, 261, doi: <https://doi.org/10.1038/s41592-019-0686-2>
- Vousden, W. D., Farr, W. M., & Mandel, I. 2016, MNRAS, 455, 1919, doi: [10.1093/mnras/stv2422](https://doi.org/10.1093/mnras/stv2422)

Wang, J. J., Graham, J. R., Pueyo, L., et al. 2016, *The Astronomical Journal*, 152, 97,

doi: [10.3847/0004-6256/152/4/97](https://doi.org/10.3847/0004-6256/152/4/97)

Wes McKinney. 2010, in *Proceedings of the 9th Python in Science Conference*, ed. Stéfan van der Walt & Jarrod Millman, 56 – 61, doi: [10.25080/Majora-92bf1922-00a](https://doi.org/10.25080/Majora-92bf1922-00a)

Zuckerman, B., Song, I., Bessell, M. S., & Webb, R. A.

2001, *ApJL*, 562, L87, doi: [10.1086/337968](https://doi.org/10.1086/337968)